Early- versus late-transition-metal-oxo bonds: the electronic structure of oxovanadium(1+) and oxoruthenium(1+)

ARTICLE *in* THE JOURNAL OF PHYSICAL CHEMISTRY · APRIL 1988

Impact Factor: 2.78 · DOI: 10.1021/j100319a005

2 AUTHORS, INCLUDING:

William A. Goddard
California Institute of Technology
1,337 PUBLICATIONS **68,337** CITATIONS

Early- versus Late-Transition-Metal–Oxo Bonds: The Electronic Structure of VO^+ and RuO^+

Emily A. Carter[†] and William A. Goddard III*

Arthur Amos Noyes Laboratory of Chemical Physics,[‡] California Institute of Technology, Pasadena, California 91125 *(Received: July 9, 1987; In Final Form: November 3, 1987)*

From all-electron ab initio generalized valence bond calculations (GVBCI-SCF) on VO^+ and RuO^+, we find that an accurate description of the bonding is obtained only when important resonance configurations are included self-consistently in the wave function. The ground state of $VO^+(^3\Sigma^-)$ has a triple bond similar to that of CO, with $D_e^{calcd}(V-O)$ = 128.3 kcal/mol [$D_e^{exptl}(V-O)$ = 1.31 ± 5 kcal/mol], while the ground state of $RuO^+(^4\Delta)$ has a double bond similar to that of O_2, with $D_e^{calcd}(Ru-O)$ = 67.1 kcal/mol. Vertical excitation energies for a number of low-lying electronic states of VO^+ and RuO^+ are also reported. These results indicate fundamental differences in the nature of the metal–oxo bond in early and late metal oxo complexes that explain the observed trends in reactivity (e.g., early metal oxides are thermodynamically stable whereas late metal oxo complexes are highly reactive oxidants). Finally, we have used these results to predict the ground states of MO^+ for other first-row transition-metal oxides.

I. Introduction

While the electronic structure of neutral transition-metal oxides has been examined by several authors,[1] the only cationic transition-metal oxide (TMO) which has been studied with correlated wave functions is[2] CrO^+. With the growing availability of experimental bond energy and reactivity data for TMO cations,[3] physical descriptions of the molecular bonding in such systems are sorely needed. Hence we have undertaken ab initio generalized valence bond (GVB) and GVBCI-SCF studies of two TMO's, VO^+ and RuO^+, as representatives of early and late transition-metal–oxo bonding, with the goal of understanding the differences in bonding and reactivity as one proceeds across the periodic table.

Examination of empirical properties of transition-metal oxides reveals that early metal–oxo compounds exhibit high stability, are relatively inert, and are characterized by very strong M–O bonds, while late TMO's tend to be highly reactive oxidizing agents with much weaker M–O bonds.[4] For example, while VO^{2+} is used as an inert ESR-active probe of protein reactive sites,[5] oxides such as CrO_3, MnO_4^-, and OsO_4 rapidly oxidize olefins and alcohols to epoxides, diols, aldehydes, ketones, and carboxylic acids.[6] Late transition-metal–oxo porphyrin complexes (models for active sites of enzymes) are effective oxygen atom transfer reagents[7] and are catalysts for hydrocarbon oxidation (cytochrome P-450 analogues).[8] The trends in reactivity are consistent with their relative thermodynamic stabilities, exemplified by the bond energies of metal–oxo diatomics (Table I). The early metal–oxo diatomics have bond strengths roughly twice as strong as their late metal counterparts. We believe that differences in the metal–oxo *bond character* are responsible for the sharp contrast in bond energies and reactivities of early and late transition-metal–oxo complexes. In the present work, we show that an oxo ligand is quite versatile: oxygen atom is capable of forming (at least) three distinct types of terminal metal–oxo bonds.[9]

Experimental data for TMO cations include thermochemical measurements to obtain bond energies and heats of formation,[3a–f] photoelectron spectra to determine the equilibrium properties of ground and excited electronic states (e.g., vibrational frequencies, bond lengths, excitation energies, and ionization potentials,[3g,h] and gas-phase studies of their chemical reactivity.[3a,i–k]

Much attention has been focused on VO^+, due to its presence in interstellar space[10] and its possible relationship to vanadium oxide catalyzed hydrocarbon oxidations.[11] Aristov and Armentrout used guided ion beam techniques to directly measure the bond energy of VO^+, obtaining $D^\circ(V^+-O)$ = 131 ± 5 kcal/mol.[3f] These authors speculated that the ground state of VO^+ might be $^3\Delta$, similar to the ground state of TiO.[1c] However Dyke et al. later recorded the photoelectron spectrum of VO,[3h] assigning the ground state of VO^+ to be $^3\Sigma^-$, with the $^3\Delta$ state lying at least

TABLE I: First-Row Transition-Metal–Oxo Bond Strengths (kcal/mol)[a]

metal	$D^\circ(M^+-O)$	$D^\circ(M-O)$	metal	$D^\circ(M^+-O)$	$D^\circ(M-O)$
Sc	159 ± 7	161.5 ± 3	Mn	57 ± 3	85 ± 4
Ti	161 ± 5	158.4 ± 2	Fe	69 ± 3	93 ± 3
V	131 ± 5	146 ± 4	Co	64 ± 3	87 ± 4
Cr	85.3 ± 1.3	110 ± 2	Ni	45 ± 3	89 ± 5

[a] From ref 3a.

[†] Present address: Department of Chemistry, University of Colorado, Boulder, CO 80309.

[‡] Contribution No. 7580.

(1) (a) Carlson, K. D.; Moser, C. *J. Chem. Phys.* **1966**, *44*, 3259. (b) Walch, S. P.; Goddard, W. A. III *J. Am. Chem. Soc.* **1978**, *100*, 1338. (c) Bauschlicher, C. W., Jr.; Bagus, P. S.; Nelin, C. J. *Chem. Phys. Lett.* **1983**, *101*, 229. (d) Bagus, P. S.; Nelin, C. J.; Bauschlicher, C. W., Jr. *J. Chem. Phys.* **1983**, *79*, 2975. (e) Bauschlicher, C. W., Jr.; Nelin, C. J.; Bagus, P. S. *J. Chem. Phys.* **1985**, *82*, 3265. (f) Nelin, C. J.; Bauschlicher, C. W., Jr. *Chem. Phys. Lett.* **1985**, *118*, 221. (g) Krauss, M.; Stevens, W. J. *J. Chem. Phys.* **1985**, *82*, 5584. (h) Bauschlicher, C. W., Jr.; Langhoff, R. S. *J. Chem. Phys.* **1986**, *85*, 5936. (i) Dolg, M.; Wedig, U.; Stoll, H.; Preuss, H. *J. Chem. Phys.* **1987**, *86*, 2123.

(2) Harrison, J. F. *J. Phys. Chem.* **1986**, *90*, 3313. $\pi \rightarrow \pi^*$ transitions using UHF (Unrestricted Hartree–Fock) wave functions for transition-metal–oxo cations have been examined by: Yamaguchi, K.; Takahara, Y.; Toyoda, Y. Fueno, T.; Houk, K. N., preprint.

(3) (a) Kang, H.; Beauchamp, J. L. *J. Am. Chem. Soc.* **1986**, *108*, 5663 and references therein. (b) Hildenbrand, D. L. *Chem. Phys. Lett.* **1975**, *34*, 352. (c) Murad, E. *J. Geophys. Res. B* **1978**, *83*, 5525. (d) Murad, E. *J. Chem. Phys.* **1980**, *73*, 1381. (e) Armentrout, P. B.; Halle, L. F.; Beauchamp, J. L. *J. Am. Chem. Soc.* **1981**, *103*, 6501. (f) Aristov, N.; Armentrout, P. B. *J. Am. Chem. Soc.* **1984**, *106*, 4065. (g) Dyke, J. M.; Gravenor, B. W. J.; Lewis, R. A.; Morris, A. *J. Chem. Soc., Faraday Trans. 2* **1983**, *79*, 1083. (h) Dyke, J. M.; Gravenor, B. W. J.; Hastings, M. P.; Morris, A. *J. Phys. Chem.* **1985**, *89*, 4613. (i) Jackson, T. C.; Jacobson, D. B.; Freiser, B. S. *J. Am. Chem. Soc.* **1984**, *106*, 1252. (j) Jackson, T. C.; Carlin, T. J.; Freiser, B. S. *J. Am. Chem. Soc.* **1986**, *108*, 1120. (k) Kang, H.; Beauchamp, J. L. *J. Am. Chem. Soc.* **1986**, *108*, 7502.

(4) Cotton, F. A.; Wilkinson, G. *Advanced Inorganic Chemistry*; Wiley: New York, 1980.

(5) (a) Selbin, J. *Coord. Chem. Rev.* **1966**, *1*, 293. (b) Chasteen, N. D.; DeKoch, R. J.; Rogers, B. L.; Hanna, M. W. *J. Am. Chem. Soc.* **1973**, *95*, 1301.

(6) Streitweiser, A., Jr.; Heathcock, C. H. *Introduction to Organic Chemistry*; MacMillan: New York, 1976.

(7) (a) Gulliver, D. J.; Levason, W. *Coord. Chem.* Rev. **1982**, *46*, 1. (b) Samuels, G. J.; Meyer, T. J. *J. Am. Chem. Soc.* **1981**, *103*, 307.

(8) (a) Collman, J. P.; Brauman, J. I.; Meunier, B.; Hayashi, T.; Kodadek, T.; Raybuck, S. A. *J. Am. Chem. Soc.* **1985**, *107*, 2000. (b) Nappa, M. J.; Tolman, C. A. *Inorg. Chem.* **1985**, *24*, 4711.

(9) Covalent metal–oxo bonding configurations for Cr, Mo, and Fe complexes have been discussed previously by: (a) Rappé, A. K.; Goddard, W. A., III *Nature (London)* **1980**, *285*, 311. (b) Rappé, A. K.; Goddard, W. A., III *J. Am. Chem. Soc.* **1980**, *102*, 5114. (c) Rappé, A. K.; Goddard, W. A., III Ibid. **1982**, *104*, 448. (d) Rappé, A. K.; Goddard, W. A., III Ibid. **1982**, *104*, 3287. (e) Goddard, W. A., III; Olafson, B. D. *Ann. N.Y. Acad. Sci.* **1981**, *367*, 419.

(10) Spinrad, H.; Wing, R. F. *Annu. Rev. Astron. Astrophys.* **1969**, *7*, 249.

0022-3654/88/2092-2109$01.50/0

1.15 eV higher in energy. From a Franck–Condon analysis of the vibrational fine structure of the $VO^+(X^3\Sigma^-) \leftarrow VO(X^4\Sigma^-)$ envelope, Dyke et al. obtained values of $\omega_e = 1060 \pm 40$ cm^{-1} and $R_e = 1.54 \pm 0.01$ Å for $VO^+(^3\Sigma^-)$. From the first ionization potential of VO (7.25 ± 0.01 eV), they derived an indirect value of $D°(V^+–O) = 138 \pm 2$ kcal/mol.

The reactivity of several metal–oxo cations (M = V, Cr, and Fe) has been studied by Freiser and co-workers[3i,j] and by Kang and Beauchamp.[3a,k] VO^+ is found to be rather unreactive, with the strongly bound oxo ligand uninvolved in the chemistry observed.[3j] In contrast, FeO^+, with its much weaker bond (Table I), is very reactive and nonselective, forming H_2O by hydrogen abstraction from alkanes.[3i,12] The reactivity of CrO^+ is intermediate in nature,[3a,k] reflecting its moderate bond strength. The oxo ligand in CrO^+ is reactive, but selective, producing aldehyde from olefins and alcohols from alkanes, without hydrogen abstraction. RuO^+ has not yet been observed experimentally.

Normally in considering how oxygen forms terminal bonds to other atoms, one thinks of double bonds consisting of one σ and one π bond (e.g., carbonyl groups within organic molecules). However, there are two other types of covalent bonding involving oxygen. First, triple bonds can be formed as in carbon monoxide, in which three valence bond (VB) resonance structures (two covalent bonds and one donor bond) participate in the bonding of $C(^3P)$ to $O(^3P)$

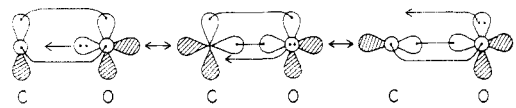

(1)

where we have indicated the locations of the valence p electrons on carbon and oxygen in eq 1.[13] Second, double bonds can be formed as in O_2, in which two VB resonance structures (one σ bond and two three-electron π bonds) contribute to the bonding between two ground state oxygen atoms (^3P).

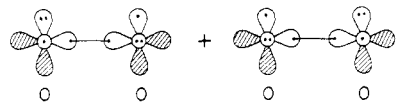

(2)

(Equivalently, molecular orbital theory describes the double bond in O_2 as filled π-bonding levels and half-filled π-antibonding levels, leading to one σ bond and two half-order bonds in the π system.)

In the two next sections, we discuss predictions for properties of VO^+ and RuO^+, drawing analogies from CO and O_2 in order to understand the variations in metal–oxo bond character. Section IV concludes with general predictions of properties and reactivity of transition-metal–oxygen bonds from a simple analysis of the expected bond character (based on the electronic state of the metal center and the nature of its ancillary ligands).

II. VO^+

The character of the metal–oxo bond depends primarily on the electronic configuration of the metal center. Since V^+ has a ground-state valence electronic configuration of $3d^4$, it has an empty d-orbital similar to the empty p-orbital of carbon (s^2p^2). As a result, oxygen forms a triple bond to V^+ in the same manner as in CO, except that the oxygen p lone pair forms the third bond by donating into an empty d-orbital on V instead of an empty p-orbital on C. The other two bonds are covalent in nature; i.e., each bond is composed of one electron from each atom. Thus, formation of the triple bond uses the $d\sigma$ and both $d\pi$ orbitals, leaving two nonbonding V electrons in the two δ orbitals. As a result, the ground state of VO^+ is $^3\Sigma^-$ (as found by Dyke[3h]).

Calculational Details. In order to treat the bonding in VO^+ properly, it is imperative to include the three possible contributing resonance structures (eq 1). This is accomplished using an MCSCF wavefunction in which all three resonance structures are optimized self-consistently at the GVB-RCI level. We begin with the GVB(3/6)-PP wave function [generalized valence bond with the perfect (singlet) pairing restriction] which allows each pair of electrons involved in each of the three bonds to be described in terms of two orbitals.[14] This allows for the motion of the two electrons within each bond to be correlated. However, of the five possible spin functions for six electrons in six different orbitals, only one is included (the perfect pairing or valence bond spin coupling). The GVB(3/6)-RCI wave function includes, for each GVB bond pair, the configurations corresponding to the three possible occupations of two electrons in two orbitals ($3^3 = 27$ configurations). This allows all possible spin couplings of the six electrons and also allows each bond pair to optimize covalent versus ionic character. The GVB(3/6)-RCI(opt) calculation solves self-consistently for the best orbitals of the RCI wave function, optimizing the spin-coupling between the electrons involved in the triple bond, the charge-transfer effects, and the interpair correlations simultaneously. The above wave functions for VO^+ and CO dissociate to HF fragments (i.e., any correlation present at R_e is gone at $R = \infty$), where the fragments are ground-state $V^+(^5D)$, $C(^3P)$, and $O(^3P)$.

In the RCI wave function, one optimized set of orbitals is used for the full wave function. However, some resonance configurations might prefer different hybridizations than others. To allow this rehybridization, we included one extra correlating orbital for each GVB bond pair (σ^*, π_x^*, and π_y^*), we allowed single excitations to these correlating orbitals from all RCI reference states [keeping the RCI(3/6)(opt) valence orbitals fixed], and we optimized these extra orbitals self-consistently. This is denoted as the RCI(3/6)*S_{corr}(opt) wave function.

The largest CI expansion, denoted RCI(3/6)(opt)*S_{val}, allowed all single excitations from all valence orbitals (excluding the oxygen and carbon 2s orbitals) to all virtual (unoccupied) orbitals for all configurations of the GVB-RCI(3/6)(opt) reference state. Such single excitations allow the shape of each orbital[15] to be modified for each resonance configuration as appropriate for its particular hybridization. This is extremely important for bond dissociation processes since the hybridization of orbitals often changes along the dissociation pathway.

The latter two wave functions dissociate to HF*S_{corr} and HF*S_{val} fragments at $R = \infty$, since all other correlations present at R_e disappear when the bond breaks. HF*S_{corr} is simply the HF wave function for the ground-state atom [single excitations to the (corresponding) correlating orbitals are optimized self-consistently, with the occupied orbitals fixed]. HF*S_{val} involves all single excitations from all valence orbitals (excluding the O and C 2s) to all virtuals from the HF wave function.

No higher levels of correlation were included beyond the CI calculations described above. For example, we did not include double excitations to virtual orbitals. This is because the bonds of VO and CO are partially donor/acceptor in character, so that a singles and doubles CI would not dissociate correctly (to be dissociation-consistent, we would need triple and quadruple excitations at R_e).

We used the Dunning valence double-ζ contraction[16] of the Huzinaga (9s5p) primitive Gaussian basis set[17] for O, augmented

(11) Sheldon, R. A.; Kochi, J. A. *Metal Catalyzed Oxidations of Organic Compounds*; Academic: New York , 1981.

(12) A preliminary study of the reactions of FeO^+ appeared earlier: Kappes, M. M.; Staley, R. H. *J. Am. Chem. Soc.* **1981**, *103*, 1286.

(13) This type of triple bond has been proposed for Cr and Mo oxo bonds by Rappé and Goddard (see ref 9). See also: (a) Allison, J. N.; Goddard, W. A., III *J. Catal.* **1985**, *92*, 127. (b) Allison, J. N.; Goddard, W. A., III *Solid State Chemistry in Catalysis*; Grasselli, R. K., Brazdil, J. F., Eds.; ACS Symposium Series No. 279f American Chemical Society: Washington, DC, 1985; pp 23–36.

(14) The details of the generalized valence bond method may be found in: (a) Hunt, W. J.; Dunning, T. H., Jr.; Goddard, W. A., III *Chem. Phys. Lett.* **1969**, *3*, 606. Goddard, W. A., III; Dunning, T. H., Jr.; Hunt, W. J. *Chem. Phys. Lett.* **1969**, *4*, 231. Hunt, W. J.; Goddard, W. A., III; Dunning, T. H. *Chem. Phys. Lett.* **1970**, *6*, 147. Hunt, W. J.; Hay, P. J.; Goddard, W. A., III *J. Chem. Phys.* **1972**, *57*, 738. Bobrowicz, F. W.; Goddard, W. A., III In *Methods of Electronic Structure Theory*; Schaefer, H. F., Ed.; Plenum: New York, 1977; pp 79–127. (b) Yaffe, L. G.; Goddard, W. A., III *Phys. Rev. A* **1976**, *13*, 1682.

(15) Carter, E. A.; Goddard, W. A., III *J. Chem. Phys.*, in press.

(16) Dunning, T. H. *J. Chem. Phys.* **1970**, *53*, 2823.

(17) Huzinaga, S. *J. Chem. Phys.* **1965**, *42*, 1293.

TABLE II: Valence Double-ζ Basis Set (Ref 19) for Vanadium: Cartesian Gaussian Functions with Exponents (α_i) and Contraction Coefficients (C_i)

type	α_i	C_i	type	α_i	C_i
s	6713.0	0.020 156 2	p	281.1	0.031 363 9
s	1013.0	0.139 572 1	p	65.29	0.195 272 4
s	228.5	0.482 309 7	p	19.81	0.520 776 1
s	62.12	0.496 741 4	p	6.575	0.432 040 0
s	88.72	−0.120 145 2	p	4.293	0.055 314 2
s	13.91	0.456 269 2	p	1.928	0.533 148 2
s	5.277	0.632 392 9	p	0.5894	0.524 511 4
s	8.688	−0.217 460 6	p	1.462	−0.228 979 1
s	1.517	0.524 631 1	p	0.09538	1.010 580 3
s	0.5481	0.608 623 6	p	0.02774	1.000 000 0
s	0.8189	−0.391 321 4			
s	0.07869	1.101 654 5	d	21.18	0.041 624 2
			d	5.566	0.204 069 9
s	0.03017	1.000 000 0	d	1.753	0.452 427 1
			d	0.5256	0.566 361 8
			d	0.1336	1.000 000 0

by one set of 3d polarization functions ($\zeta^d = 0.95$),[18] and the Rappé and Goddard valence double-ζ basis set for vanadium (Table II).[19] The ground-state bond distance and the vertical excitation energies were optimized at the RCI(3/6)(opt) level.

Results. The ground state of VO^+ is predicted to be $^3\Sigma^-$, with a bond length of $R_e(V^+–O) = 1.56$ Å and a harmonic frequency of $\omega_e = 1108$ cm^{-1}, in excellent agreement with the experimental results of Dyke et al. [$R_e(V^+–O) = 1.54 \pm 0.01$ Å and $\omega_e = 1060 \pm 40$ cm^{-1}].[3h] Two of the four d electrons on V are involved in bonding to the oxygen, with the remaining two nonbonding d electrons in δ orbitals (to reduce electron repulsion). The bond character is found to be a triple bond, but Mulliken population analysis (1.46 electrons in each oxygen pπ orbital and 1.33 electrons in the oxygen pσ orbital) suggests that the two resonance structures of eq 1 having covalent σ bonds (with an average of 1.5 electrons in each O pπ orbital and 1.0 electron in the O σ orbital) dominate the bonding. If each of the three resonance structures contributed equally, each oxygen p orbital would have an occupation of $1^1/_3$ electrons. Thus, the bonds in VO^+ are best viewed as one covalent σ bond, one covalent π bond, and one donor/acceptor π bond

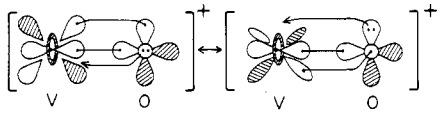

(3)

with 0.33 electron transferred from V^+ to O in the σ system and 0.07 electron transferred back to V^+ in the π system. This is consistent with the net charge of −0.26 electron on oxygen. Similarly, Mulliken population analysis of CO finds 1.22 electrons in O pσ and 1.46 electrons in each O pπ. Therefore, although all three resonance structures participate to some degree in both VO^+ and CO, the dominant resonance structures are those involving covalent σ bonding. The GVB-RCI(3/6)(opt) orbitals for VO^+ and CO are compared in Figure 1, where we see that the bonding in CO and VO^+ is indeed very similar.[20]

The triple bond character for both VO^+ and CO results in very strong bonds. Table III compares their bond strengths as a

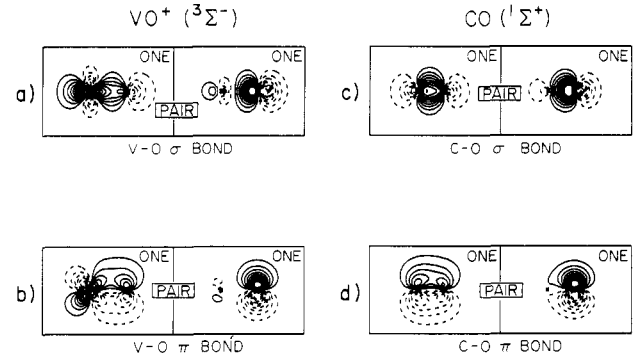

Figure 1. The GVB one-electron orbitals for the σ and one π bond (the other is identical) of $VO^+(^3\Sigma^-)$ and $CO(^1\Sigma^+)$: (a) the V–O σ bond; (b) the V–O π bond; (c) the CO σ bond; and (d) the CO π bond. Contours are from −0.6 to 0.6 au incremented by 0.06 au.

function of increasing electron correlation. The correlation problem is much more severe for transition metals than for organic molecules, as is indicated by the disparity between the Hartree–Fock (HF) and the experimental values for D_e [$\Delta D_e(VO^+) = 142$ kcal/mol, whereas $\Delta D_e(CO) = 88$ kcal/mol]. VO^+ is unbound by 11 kcal/mol at the HF level, due to the inability of HF theory to describe the low overlap (π) bonds present in multiply bonded metal–ligand complexes.[21] Once static electron correlation is built into the wave function (GVB-PP), properly describing the low overlap π bonds ($S_\pi = 0.7$), VO^+ is stabilized by almost 60 kcal/mol. Another large increase in stability occurs at the RCI level (53 kcal/mol more stable than GVB-PP) in which proper spin coupling (important for high spin metal atoms)[21] and all three resonance structures are taken into account.

Including self-consistent optimization of the resonance and spin-coupling effects, along with single excitations to virtual orbitals to account for orbital shape changes along the dissociation pathway, leads to bond energies close to experiment for both CO (theory, 249 kcal/mol; experiment, 258 kcal/mol[22]) and VO^+ (theory, 119 kcal/mol; experiment, 131 ± 5 kcal/mol[3f]). Since the bonding is very similar in CO and VO^+, we expect that the correlation energy beyond our current calculations should be similar. Thus, using $\Delta_{corr} = D_e^{exptl}(CO) - D_e^{calcd}(CO) = 9.6$ kcal/mol at the highest level of correlation, RCI(3/6)(opt)*S_{val}, we estimate the exact VO^+ bond strength by adding Δ_{corr} to $D_e(VO^+)$ at the same level of theory. This yields our best estimate for the V–O bond energy, 118.7 + 9.6 = 128.3 kcal/mol, in excellent agreement with the experimental value of 131 ± 5 kcal/mol.[3f]

Finally, we examined two other triplet states at the predicted equilibrium bond distance for the ground $^3\Sigma^-$ state ($R_e = 1.56$ Å). We find a vertical excitation energy of 40.7 kcal/mol to the $^3\Delta$ state, which has a CO-type bond with only one resonance structure.

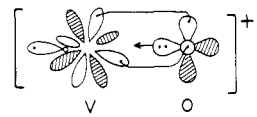

(4)

Two d electrons on V^+ form π bonds to oxygen, with the nonbonding electrons residing in δ and σ orbitals. The large vertical state splitting may be understood in terms of the difference in bond character between the $^3\Sigma^-$ and $^3\Delta$ states. While the $^3\Sigma^-$ ground state forms one donor π bond, one covalent σ bond, and one covalent π bond, the $^3\Delta$ state is forced to form two covalent π bonds and one donor σ bond. Covalent π bonds are weak relative to covalent σ bonds, with the small 3d orbitals of V^+ enhancing this effect. Thus, the bond in the $^3\Delta$ state is weaker than in the ground state because of the tradeoff between covalent σ and π bonds. However, if the 3d orbitals were more diffuse so that

(18) The oxygen d exponent was optimized for H_2O by: Bair, R. A.; Goddard, W. A., III, unpublished results.

(19) (a) Rappé, A. K.; Goddard, W. A., III, to be submitted for publication. This basis set was optimized for the d^n configuration of the metal as discussed in: Rappé, A. K.; Smedley, T. A.; Goddard, W. A., III *J. Phys. Chem.* **1981**, *85*, 2607. (b) The HF ^5F–^5D state splitting for V^+ with this basis is 7.3 kcal/mol, which may be compared with the numerical Hartree–Fock value of −3.5 kcal/mol (Martin, R. L.; Hay, P. J. *J. Chem. Phys.* **1981**, *75*, 4539) and the experimental value (averaged over J states) of 7.6 kcal/mol (Moore, C. E. *Atomic Energy Levels*; NSRDS-NBS-35, 1971).

(20) We obtained one-electron orbitals from the RCI-MCSCF natural orbitals by freezing all orbitals other than GVB pairs and recalculating the GVB-PP CI coefficients with which to transform the natural orbitals to one-electron GVB orbitals. (No mixing is allowed between GVB pairs.)

(21) Carter, E. A.; Goddard, W. A., III *J. Phys. Chem.* **1984**, *88*, 1485.

(22) Huber, K. P.; Herzberg, G. *Constants of Diatomic Molecules*; Van Nostrand: New York, 1979.

TABLE III: Comparison of Adiabatic Bond Energies (D_e) for VO^+ and CO (kcal/mol)[a]

calculation	total energies, hartrees			$D_e(V^+{\equiv}O)$[c]	$D_e(C{\equiv}O)$[d]
	$VO^+(^3\Sigma^-)$	$CO(^1\Sigma^+)$	$O(^3P)$[b]		
HF	−1016.388 80 (1/1)	−112.757 12 (1/1)	−74.800 59 (1/1)	−11.1	170.6
GVB(3/6)-PP	−1016.480 99 (6/6)	−112.818 49 (6/6)	−74.800 59 (1/1)	46.8	209.1
GVB-RCI(3/6)	−1016.565 30 (27/126)	−112.877 21 (27/37)	−74.800 59 (1/1)	99.7	246.0
GVB-RCI(3/6)(opt)	−1016.578 23 (27/126)	−112.879 09 (27/37)	−74.800 59 (1/1)	107.8	247.2
RCI(3/6)*S_{corr}(opt)	−1016.590 51 (81/582)	−112.881 98 (81/139)	−74.801 48 (5/9)	115.0	248.4
RCI(3/6)(opt)*S_{val}	−1016.596 66 (747/4778)	−112.883 43 (351/649)	−74.801 61 (33/53)	118.7	249.2
$D_e + \Delta_{corr}$[g]				128.3	(258.8)
experiment				131 ± 5[e]	258.8[f]

[a] Calculational details are given in section II. The corresponding number of spatial configurations/spin eigenfunctions for each wave function is listed in parentheses after each total energy. [b] Total energies for ground-state $O(^3P)$ are calculated at the level consistent for $R = \infty$ for each calculation: HF, HF*S_{corr}, and HF*S_{val}. [c] The wave functions for VO^+ all dissociate to HF ground-state $V^+(^5D)$ (total energy = −941.605 84 hartrees). [d] The wave functions for CO all dissociate to HF ground-state $C(^3P)$ (total energy = −37.684 62 hartrees). [e] Reference 3f. [f] Reference 22. [g] $\Delta_{corr} = D_e^{expt}(CO) - D_e^{calcd}(CO) = 9.6$ kcal/mol.

TABLE IV: GVBCI(opt) Vertical Excitation Energies for RuO^+ at $R_e(^4\Delta\ RuO^+) = 1.75$ Å (kcal/mol)[a]

state	character[b]	atomic valence electron config: O σ	O π_x	O π_y	Ru^+ σ	Ru^+ π_x	Ru^+ π_y	Ru^+ δ_{xy}	Ru^+ $\delta_{x^2-y^2}$	total energy, hartrees	ΔE
$^2\Delta$	**($^1\Sigma^+$ bond) × (Ru δ^3)** + low-spin ($^3\Sigma^-$ bond) × (Ru δ^3)	↓	2	↑	↑	↓	2	2	↑	−4511.976 15	37.1
$^2\Sigma^+$	CO-type bond	2	↑	↑	↑	↓	↓	2	2	−4511.987 88	29.7[c]
$^2\Sigma^+$, $^2\Sigma^-$	($^1\Delta$ bond) × (Ru δ^3)	↓	2	↑	↑	↓	2	2	↑	−4511.991 87	27.2
$^2\Delta$	**low-spin ($^3\Sigma^-$ bond) × (Ru δ^3)** + ($^1\Sigma^+$ bond) × (Ru δ^3)	↓	2	↑	↑	↑	2	2	↓	−4512.002 39	20.6
$^2\Gamma$	($^1\Delta$ bond) × (Ru δ^3)	↓	2	↑	↑	↓	2	2	↑	−4512.008 28	16.9
$^4\Delta$	high-spin ($^3\Sigma^-$ bond) × (Ru δ^3)	↓	2	↑	↑	↑	2	2	↑	−4512.035 21	0.0

[a] Calculational details are given in section III. [b] Character of each state describes the coupling between the Ru nonbonding electrons (δ^3) and the Ru–O bond (described by the analogous state of O_2 to indicate the type of Ru–O bond). The dominant character for each $^2\Delta$ state is shown in boldface. [c] The consistent calculation for the CO-type bond in RuO^+ is the RCI(2/4)(opt) calculation described in ref 28.

stronger π bonds could be formed (due to higher overlap), then the $^3\Delta$ state might be competitive. Indeed, the ground state of the isoelectronic TiO is $^3\Delta$,[1c,22] perhaps because the covalent π bonds are stronger for Ti(0) than for V(I).

A $^3\Phi$ state is found to be only 1.9 kcal/mol above the $^3\Delta$ state, with a nonbonding electron configuration of $\delta^1\pi^1$. This state has only a double bond between V^+ and O due to the presence of three electrons in one of the π planes.

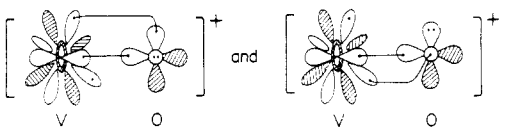

(5)

These vertical excitation energies are considerably higher than the 1.15 eV found by Dyke et al.[3h] from the peak to peak distances in the photoelectron spectrum of VO. However, we believe that the first IP of VO may be lower in energy than 7.25 eV as reported by Dyke, since the bond energy Dyke derives for VO^+ (137.9 ± 2.3 kcal/mol) is higher than the directly measured value (131 ± 5 kcal/mol)[3f] by ~7 kcal/mol. The direct VO^+ bond energy implies an adiabatic IP for VO of 6.95 eV (7 kcal/mol lower than Dyke's 7.25 eV), resulting in a higher experimental $^3\Delta$–$^3\Sigma^-$ state splitting for VO^+ (33 ± 5 kcal/mol), in closer agreement with the theory (40.7 kcal/mol). However, an analysis of the ionization thresholds and an optimization of the excited-state potential curves are necessary for any quantitative statement concerning adiabatic state splittings. Since we are primarily concerned with ground-state properties of metal oxides, we will eschew this issue for the present.

III. RuO^+

Group VIII transition metals have doubly occupied d orbitals for all low-lying electronic states. The lack of empty d orbitals decreases the favorability of forming triple bonds to oxygen (unless ancillary ligands put the metal in a low-spin electronic state). The presence of doubly occupied d orbitals makes "metallaketone" structures with covalent σ and π bonds unlikely due to electron–electron repulsion between a doubly occupied metal dπ orbital and the doubly occupied oxygen pπ orbital. For Ru, the large 4dπ orbital overlaps the O 2pπ orbital to such an extent that the "metallaketone" type of double bond is 16.9 kcal/mol higher in energy than the ground state.

We find that RuO^+ has neither a triple bond nor a traditional olefinic double bond, but rather a biradical double bond analogous to the bond in O_2. Four of the d electrons in high-spin d^7 Ru^+ are involved in the $^3\Sigma^-$-type bonding to oxygen (as in ground-state O_2), forming a covalent σ bond and two three-electron π bonds.

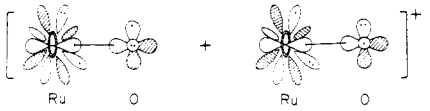

(6)

Since the Ru dσ and dπ orbitals are involved in bonds to oxygen, the other three Ru 4d electrons occupy the dδ orbitals. High spin coupling of the $^3\Sigma^-$ Ru–O bonding and the δ^3 nonbonding electrons on Ru gives rise to the ground $^4\Delta$ state. However, just as in O_2, there are other low-lying electronic states ($^1\Delta_g$ and $^1\Sigma_g^+$ for O_2) with resonance structures containing conventional double bonds (one σ and one π). These O_2-type bonding configurations, when coupled high spin or low spin to the δ^3 Ru electrons, give rise to the spectrum of states shown in Table IV.

Calculational Details. The resonance present in RuO^+ necessitates an MCSCF treatment similar to VO^+ in which both resonance structures of eq 6 are optimized self-consistently. This GVBCI(opt) calculation consists of a self-consistent RCI(1/2) treatment of the Ru–O σ bond, a full six-electron CI among the four orbitals of the Ru–O π system and simultaneous inclusion of the two possible configurations of the three electrons in the Ru δ orbitals. The GVBCI(opt) wave function, with its full CI in the π system, is capable of describing any electronic state that is determined by the occupation and spin-coupling of the π orbitals. Thus the vertical excitation energies to just such states (bonds analogous to the $^3\Sigma_g^-$, $^1\Delta_g$, and $^1\Sigma_g^+$ states of O_2) were calculated at this level (Table IV).

One higher level MCSCF calculation was performed in which the valence orbitals from the GVBCI(opt) calculation were kept fixed, while allowing single $\pi \rightarrow \pi^*$, $\delta \rightarrow \delta^*$, $\sigma \rightarrow \sigma^*$ excitations from the GVBCI reference states. This GVBCI*S_{corr}(opt) calculation optimizes the shapes of seven important, low-lying correlating orbitals (with σ_{z^2}, π_{ux}, π_{uy}, π_{gx}, π_{gy}, δ_{xy}, and $\delta_{x^2-y^2}$ sym-

metries). Moss and Goddard used an analogous CI treatment to accurately predict the bond energy and the electronic state spectrum of O_2.[24] (They obtained D_e = 112.5 kcal/mol in comparison to the experimental value of 120.2 kcal/mol.[22])

Three CI calculations involving excitations to the whole virtual space were performed. First, single excitations from all valence orbitals (excluding the oxygen 2s) to all virtuals from the GVBCI(opt) wave function, GVBCI(opt)*S_{val}, allows the orbital shape changes important during bond rupture. Second, the presence of a covalent σ bond allows a dissociation consistent[15,21,25,26] calculation to be performed, in which all single and double excitations from the σ bond pair to all virtuals are allowed from the GVBCI reference states. This CI incorporates full correlation of the two electrons involved in the breaking bond. We carried out these single and double excitations (using the GVBCI reference states) from both the GVBCI*S_{corr}(opt) wave function (denoted GVBCI*[S_{corr} + SD_σ]) and from the GVBCI(opt) wave function, where singles from the Ru 4d and O 2p valence space were also allowed (denoted GVBCI(opt)*[S_{val} + SD_σ]). This latter wave function has been shown to yield bond energies accurate to 1–5% for both organic and organometallic molecules.[15,21,26]

The wave functions described above dissociate to ground-state $Ru^+(^4F)$ and ground-state $O(^3P)$. The HF, GVB(1/2)PP, and GVBCI(opt) wave functions dissociate to HF fragments. The wave functions involving optimization of correlating orbitals dissociate to HF*S_{corr}, while the wave functions involving single excitations to virtuals from the valence space (excluding the O 2s) dissociate to HF*S_{val} (see section II). (Note that single and double excitations out of the breaking bond pair dissociate to just singles out of a singly occupied orbital on each fragment.)

We used the same oxygen basis as described in section II, along with the Rappé and Goddard valence double-ζ basis for Ru.[19a,26a] The Ru–O bond length was optimized for the ground $^4\Delta$ state at the GVBCI(opt) level.

Results. The ground state of RuO^+ is predicted to be $^4\Delta$, with an equilibrium bond length of R_e = 1.75 Å and an equilibrium vibrational frequency of ω_e = 787 cm^{-1}. Although RuO^+ has not yet been observed, these values may be compared with those of a terminal Ru=O porphyrin complex, where the bond length is 1.765 Å and the Ru=O stretching frequency is 855 cm^{-1}.[27] The Ru=O bond is very covalent, with little charge transfer (0.04 electron) to the metal (from Mulliken population analysis). The GVB-CI(opt) orbitals for both RuO and O_2 are shown in Figure 2, where we see that the Ru–O σ bond is just as covalent as the O–O σ bond. The three-electron π systems of both RuO^+ and O_2 are very similar, with the Ru–O π_u and π_g orbitals delocalized over both centers as in O_2.

The vertical electronic state spectrum shown in Table IV reveals the same ordering of bond types as in O_2, with the $^4\Delta$ state ($^3\Sigma^-$ biradical bonding) lowest in energy, followed by the $^2\Gamma$ state [$^1\Delta$ metallaketone bonding (i.e., covalent σ and π bonds)] 16.9 kcal/mol up. This 1Δ–$^3\Sigma^-$ splitting of 16.9 kcal/mol for RuO^+ may be compared with the $^1\Delta_g$–$^3\Sigma_g^-$ splitting of 22.6 kcal/mol for O_2.[22] The energy splitting between these two states corresponds to twice the exchange term between the singly occupied π_{gx} and π_{gy} orbitals, K_{xy}; thus we find $K_{xy}(RuO^+)$ = 8.45 kcal/mol and $K_{xy}(O_2)$ = 11.3 kcal/mol. For a covalent bond, this exchange term should be about half of the (average) atomic exchange energy (K_{pp} = 25.4 kcal/mol for O and K_{dd} = 14.6 kcal/mol for Ru^+). Since $K_{xy}(O_2)$ = 11.3 kcal/mol and $K_{xy}(RuO^+)$ = 8.5 kcal/mol, this is approximately correct.

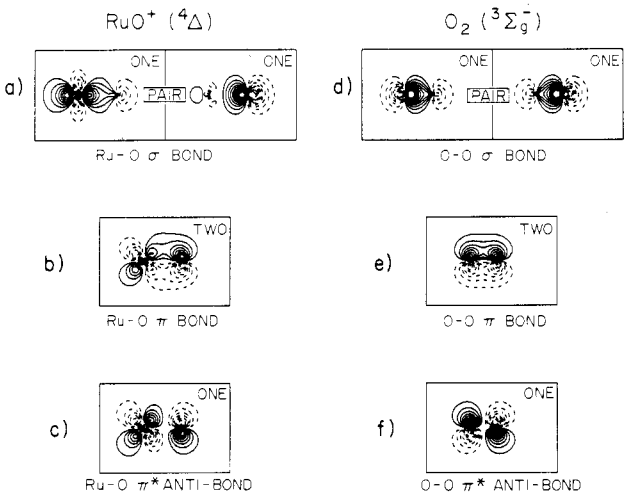

Figure 2. The GVB one-electron orbitals for the σ bond, a doubly occupied π orbital, and a single occupied π^* orbital of $RuO^+(^4\Delta)$ and $O_2(^3\Sigma_g^-)$: (a) the Ru–O σ bond; (b) an Ru–O π orbital; (c) an Ru–O π^* orbital; (d) the O_2 σ bond; (e) an O_2 π_u orbital; and (f) an O_2 π_g^* orbital. Contours are from −0.6 to 0.6 au incremented by 0.06 au.

The $^2\Delta$ state with the $^1\Sigma^+$ bonding configuration should be $\sim 4K_{xy}$ = 34 kcal/mol higher in energy than the $^3\Sigma^-$ bonding ground state. Indeed, we find it at 37.1 kcal/mol above $^4\Delta$! A lower $^2\Delta$ state, along with a nonequilibrium bond length, destabilizes the high-lying $^2\Delta$ state. In sum, the ordering of states in the O_2-type manifold is determined by a combination of two factors: (i) lower electron–electron repulsion favors $^3\Sigma^-$ over $^1\Delta$ and $^1\Delta$ over $^1\Sigma^+$ and (ii) high-spin coupling between the Ru–O bond and the nonbonding δ^3 electrons is favored over low-spin coupling. Thus the low-lying states which have O_2-type bonds are (in order of increasing energy): $^4\Delta$, $^2\Gamma$, $^2\Delta$, $^2\Sigma^\pm$, and $^2\Delta$.

We also calculated the energy of the state of $RuO^+(^2\Sigma^+)$ having a CO-type triple bond (it has a nonbonding $d\delta^4$ configuration on Ru^+). This state involves only one resonance structure of eq 1

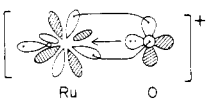

(7)

since the other resonance structures would require promotion of Ru^+ to an intermediate spin s^1d^6 excited state. (We did not investigate $^2\Pi$ CO-type bonding, in which three electrons in one π plane would destroy the triple bond.) While eq 7 has three electrons in the σ system, the triple bond may still form, since $d\sigma$ orbitals rehybridize away from the donor bond more easily (mixing in s character) than $d\pi$ orbitals (mixing in higher energy p character). At the GVB-RCI(2/4)(opt) level,[28] this state lies 29.7 kcal/mol above the ground state. As expected, the lack of empty d orbitals on the metal destabilizes triple bonds to oxygen, and the biradical double bond is preferred.

The bond energies for the ground state of $RuO^+(^4\Delta)$ and the ground state of $O_2(^3\Sigma_g^-)$ are shown in Table V as a function of increasing electron correlation. We see that HF and GVB-PP are inadequate descriptions of metal–ligand multiple bonds. Although only a valence level calculation, the GVBCI(opt) description stabilizes both RuO^+ and O_2 considerably. As single and (selected dissociation-consistent) double excitations are included in the wave function, we converge to a bond energy for O_2 of 115.5 kcal/mol at the GVBCI(opt)*[S_{val} + SD_σ] level, 4.7 kcal/mol lower than the experimental value of 120.2 kcal/mol.[22]

(23) Deleted in proof.

(24) Moss, B. J.; Goddard, W. A., III *J. Chem. Phys.* **1975**, *63*, 3523.

(25) (a) Bair, R. A.; Goddard, W. A., III, unpublished work. (b) Bair, R. A. Ph.D. Thesis, California Institute of Technology, 1981.

(26) (a) Carter, E. A.; Goddard, W. A., III *J. Am. Chem. Soc.* **1986**, *108*, 2180. (b) Carter, E. A.; Goddard, W. A., III *J. Am. Chem. Soc.*, submitted for publication. (c) Carter, E. A. Goddard, W. A., III *Organometallics*, in press.

(27) (a) Che, C.-M.; Wong, K.-Y.; Mak, T. C. W. *J. Chem. Soc., Chem. Commun.* **1985**, *546*. (b) Che, C.-M.; Tang, T.-W.; Poon, C.-K. *J. Chem. Soc., Chem. Commun.* **1984**, 641.

(28) The $RuO^+(^2\Sigma^+)$ state has CO-type bonding with two GVB π pairs (two natural orbital per pair) but with three σ electrons shared between the Ru $d\sigma$ and O $p\sigma$ orbitals. We solved for this state self-consistently using the GVB-RCI(2/4)(opt) wave function which allows both occupations of the two σ orbitals (an MCSCF calculation with 3 × 3 × 2 = 18 spatial configurations). This level of calculation maintains the same degrees of freedom (e.g., the same number of orbitals and the same correlations) as the GVBCI(opt) wave function for the O_2-type bonding in RuO^+, so that the two states are treated consistently.

TABLE V: Comparison of Adiabatic Bond Energies (D_e) for RuO^+ ($^4\Delta$) and $O_2(^3\Sigma_g^-)$ (kcal/mol)[a]

calculation	total energies, hartrees				D_e (Ru^+=O)	D_e (O=O)
	$RuO^+(^4\Delta)$	$O_2(^3\Sigma_g^-)$	$Ru^+(^4F)$[b]	$O(^3P)$[b]		
HF	−4511.913 27 (1/1)	−149.628 55 (1/1)	−4437.183 54 (1/1)	−74.800 59 (1/1)	−44.5	17.2
GVB(1/2)-PP	−4511.962 79 (2/2)	−149.656 63 (2/2)	−4437.183 54 (1/1)	−74.800 59 (1/1)	−13.4	34.8
GVBCI(opt)	−4512.035 21 (22/40)	−149.734 56 (6/10)	−4437.183 54 (1/1)	−74.800 59 (1/1)	32.1	83.7
GVBCI*S_{corr}(opt)	−4512.076 10 (288/916)	−149.778 79 (54/130)	−4437.184 29 (5/11)	−74.801 48 (5/9)	56.7	110.3
GVBCI(opt)*S_{val}	−4512.080 99 (1218/3964)	−149.781 38 (154/390)	−4437.184 50 (21/48)	−74.801 61 (33/53)	59.5	111.8
GVBCI*[S_{corr}(opt) + SD_σ]	−4512.083 16 (1990/5300)	−149.785 71 (378/846)	−4437.184 29 (5/11)	−74.801 48 (5/9)	61.1	114.7
GVBCI(opt)*[S_{val} + SD_σ]	−4512.085 49 (2656/7616)	−149.787 36 (426/966)	−4437.184 50 (21/48)	−74.801 61 (33/53)	62.4	115.5
$D_e + \Delta_{corr}$[d]					67.1	(120.2)
experiment						120.2[c]

[a] Calculational details are given in section III. The associated number of spatial configurations/spin eigenfunctions for each calculation is given in parentheses after each total energy. [b] Total energies for the fragments are calculated at levels consistent for $R = \infty$ for each calculation (section III). [c] Reference 22. [d] $\Delta_{corr} = D_e^{expt}(O_2) - D_e^{calcd}(O_2) = 4.7$ kcal/mol.

TABLE VI: Comparison of Properties of VO^+ and RuO^+

property	VO^+		RuO^+	
	theory[a]	expt	theory[a]	expt
ground state	$^3\Sigma^-$	$^3\Sigma^-$[b]	$^4\Delta$	
bond order	3	3[c]	2	
net charge on oxygen[d]	−0.26		+0.04	
R_e, Å	1.56	1.54 ± 0.01[b]	1.75	1.765[e]
ω_e, cm^{-1}	1108	1060 ± 40[b]	787	855[e]
D_e, kcal/mol	128.3	131 ± 5[c]	67.1	

[a] This work. [b] Reference 3h. [c] Reference 3f. [d] Based on Mulliken populations of the RCI(opt) for VO^+ and GVBCI(opt) for RuO^+ wave functions. [e] The experimental R(Ru=O) and ω(Ru=O) are from a Ru=O porphyrin complex (ref 27).

The analogous calculation on RuO^+ yields $D_e(Ru^+{=}O) = 62.4$ kcal/mol. Using $\Delta_{corr}(O{=}O) = 4.7$ kcal/mol, we estimate $D_e^{exact}(Ru^+{=}O) = 67.1$ kcal/mol as our best estimate for the bond energy of RuO^+. An experimental bond energy of RuO^+ is not known; however, this value is close to the measured bond energy of FeO^+ [$D°(Fe^+{=}O) = 69 \pm 3$ kcal/mol].[3e]

IV. Discussion and Summary

The contrasts in ground-state properties of VO^+ and RuO^+ (Table VI) provide prototypes for the differences in bonding and reactivity between early and late transition-metal–oxo cations. The early metal forms a CO-type triple bond with no unpaired electrons on the oxygen ligand, while the late metal forms a biradical O_2-type double bond with one unpaired electron on the oxo group. For maximum bonding, the early metal requires two singly occupied and one empty d orbitals. For maximum bonding, the late metal requires single occupied dσ and dπ orbitals and a doubly occupied dπ orbital. The charge on oxygen in the two systems reflects the tendency toward ionic bonding (M^+O^-) for early metal oxides and toward more covalent structures for the late metal oxo compounds. The equilibrium properties of the ground state of VO^+ are in excellent agreement with the values derived from the photoelectron spectrum of VO.[3h] The ground-state properties for RuO^+ are in accord with both RuO porphyrin complexes[27] and FeO^+.[3e,i] The early metal oxide is characterized by a bond nearly twice as strong as the late metal oxide, with vibrational frequencies and bond lengths commensurate with their relative bond strengths.

These contrasts in properties predicted for the simple metal–oxo diatomics are consistent with known reactivity and stability trends. The triply bonded oxygen of VO^+ has no unpaired electrons on the oxygen and hence is relatively inert. Freiser and co-workers[3j] observed precisely this behavior, with the oxo ligand unreactive toward a variety of hydrocarbon substrates. Further testimony of the unreactive nature of triply bonded metal–oxos is provided by the vanadyl cation, VO^{2+}, which is used as an ESR-active probe of proteins because it does not react with substrates.[5] On the other hand, we expect RuO species to be reactive due to the radical character on the oxygen. Consistent with this hypothesis, isoelectronic FeO complexes are known to oxidize hydrocarbons to alcohols,[8b] FeO^+ in the gas phase forms H_2O from reaction with alkanes,[3i,12] RuO bipyridyl complexes are active oxygen atom transfer catalysts,[7] and RuO_4 is an exceedingly powerful oxidizing agent.[4] Sample reactions expected for RuO/FeO systems are as follows.

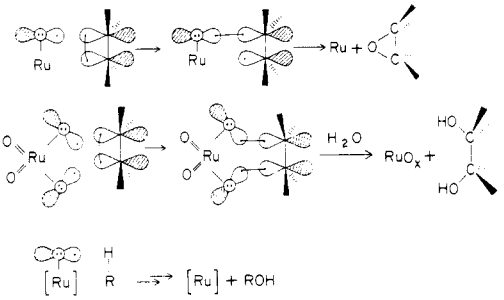

(8)

Based on the M–O bond character, one can partition the terminal transition metal oxides into three groups:

(i) The early transition metals (e.g., Sc, Ti, and V) have empty d orbitals, and hence can form triple bonds (CO-type) in which all four of the O electrons are paired up with the metal, rendering the oxygen inert. This requires that there be two electrons distributed among the (three) metal dσ and dπ orbitals. Thus $Sc^+(11000)$, $Ti^+(11100)$, $V^+(11110)$ (and Ti^{2+}, V^{2+}, Cr^{3+}, V^{3+}, ...) can all have maximum bonding [valence d-electron configurations (dσ dπ_x dπ_y dδ_{xy} d$\delta_{x^2-y^2}$) are shown in parentheses].

(ii) The $Cr^+(11111)$ and $Mn^+(s^1 11111)$ triads have no empty d orbitals and no doubly occupied d orbitals. As a result, these metals tend to form conventional double bonds involving one σ and one π bond and are expected (and found experimentally[3a]) to be moderate in their reactivity.[29]

(iii) The group VIII metals cannot readily form triple bonds since they have no empty d orbitals to overlap the oxygen lone pair. However, the group VIII metals can form the very reactive, biradical O_2-type double bonds since they have doubly occupied d orbitals available for the π resonance. This requires two singly occupied orbitals (dσ, dπ) and a doubly occupied dπ orbital. Thus d^6, d^7, and d^8 ions (e.g., Fe^{2+}, Ru^+, and Co^+) can all achieve maximum bonding.

Thus the reactivity of metal–oxo systems can be understood by considering how the d-orbital occupation on the metal dictates the type of metal–oxygen bond formed, with early metals forming strong, unreactive triple bonds and late metals forming weak, reactive biradical double bonds.

These predictions for the ground states of MO^+ are summarized in Table VII. Taking the d^n configuration of M^+ (or M^{2+}) as the starting point leads to one set of predictions. This column would be relevant for a metal in a porphyrin environment (for M^{2+}) and for elements of the second transition row. For the first and third transition rows, s^1d^{n-1} configurations may be more

(29) Oxidizing the metals from the Cr or Mn triads (Cr^{2+}, Mn^{3+}) results in vacant metal d orbitals and hence can allow formation of triple bonds. See ref 9.

TABLE VII: Electronic States and Spatial Configurations for MO^+

		$d^n M^+$				$s^1d^{n-1} M^+$			
	bond energy, kcal/mol	bond order	MO^+ config $\sigma\ \pi$	δ	sym	bond order	MO^+ config $\sigma\ \pi$	δ s	sym
ScO^+	159 ± 7	3[a]	2 22	00	$^1\Sigma^+$				
TiO^+	161 ± 5	3[a]	2 22	10	$^2\Delta$				
VO^+	131 ± 5	3[a]	2 22	11	$^3\Sigma^-$				
CrO^+	85 ± 1	$2^1/_2$	2 32	11	$^4\Pi$				
MnO^+	57 ± 3	2[b]	2 33	11	$^5\Sigma^+$	$2^1/_2$	2 32	11 1	$^5\Pi$
FeO^+	69 ± 3	2[b]	2 33	21	$^4\Delta$	2[b]	2 33	11 1	$^6\Sigma^+$
CoO^+	64 ± 3	2[b]	2 33	22	$^3\Sigma^-$	2[b]	2 33	21 1	$^5\Delta$
NiO^+	45 ± 3	$1^1/_2$	2 43	22	$^2\Pi$	2[b]	2 33	22 1	$^4\Sigma^-$

[a] Triple bond as in VO^+. [b] σ bond plus the two three-electron π bonds as in RuO^+.

relevant. This does not lead to different predictions for configurations for the early metals but leads to a second set of possible ground configurations for the late metals, as indicated in the second column of Table VII. Special points to note are as follows:

(a) ScO^+, TiO^+, and VO^+ can form strong triple bonds (with 0, 1, or 2 electrons in δ orbitals) with symmetries $^1\Sigma^+$, $^2\Delta$, and $^3\Sigma^-$, respectively, but CrO^+ ($^4\Pi$) necessarily has an electron in an antibonding orbital, leading to much weaker bonding.

(b) For MnO^+, one would expect a molecular configuration related to s^1d^5 Mn^+ and hence a $^5\Pi$ state. Close in energy should be a $^5\Sigma^+$ state, derived from the d^6 configuration of Mn^+, forming an O_2-type bond to oxygen atom.

(c) The ground state of FeO^+ is expected to differ from that found for RuO^+ in section III. Instead of the $^4\Delta$ ground state found for RuO^+, we expect a $^6\Sigma^+$ ground state for FeO^+. This change in electronic states may be understood simply in terms of the change in ground state of the metal ions, with the s^1d^6 ground state of Fe^+ and the d^7 ground state of Ru^+ leading to O_2-type bonds of $^6\Sigma^+$ and $^4\Delta$ symmetries, respectively (the nonbonding d electrons on Fe^+ having a preferred configuration of $\sigma^1\delta^1\bar{\delta}^1$, while the s and three $d\pi$ electrons comprise the O_2-type bond).

(d) CoO^+ should have a low-lying excited state of $^5\Delta$ symmetry and a ground state of $^3\Sigma^-$ symmetry, arising from O_2-type bonds to oxygen to the s^1d^7 excited state and the d^8 ground state of Co^+. The $^5\Delta$ excited state of CoO^+ has an extra δ electron compared with $FeO^+(^6\Sigma^+)$, while the $^3\Sigma^-$ ground state of CoO^+ has both δ orbitals doubly occupied.

(e) NiO^+ is predicted to have a $^2\Pi$ ground state involving the d^9 ground state of Ni^+ forming a single σ bond to oxygen (with an unpaired π electron left on O), with a $^4\Sigma^-$ excited state derived from an O_2-type bond to the s^1d^8 excited state of Ni^+. The low bond energy of NiO^+ (45 kcal/mol) is consistent with the formation of a single bond as in $^2\Pi$ NiO^+.

(f) As a final note, ligand field effects in porphyrins should yield d^n ground states for M^{2+}. Thus the electronic states of MO^{2+} in porphyrins should correspond to the lowest electronic state predicted for d^n MO^+, namely, a $^4\Delta$ ground state for FeO^+, while CoO^+ (porph) and NiO^+ (porph) should have $^3\Sigma^-$ and $^2\Pi$ ground states, respectively.

Acknowledgment. This work was supported by the National Science Foundation (Grant No. CHE83-18041) with some support from the Shell Companies Foundation. E.A.C. acknowledges a National Science Foundation predoctoral fellowship (1982–1985), a research grant award from the International Precious Metals Institute and Gemini Industries (1985–1986), and a SOHIO fellowship in Catalysis (1986–1987).

Registry No. VO^+, 12192-26-6; RuO^+, 113110-48-8.

Anisotropic Polarizability Density in the H_2^+ Molecule

David H. Drum and William H. Orttung*

Department of Chemistry, University of California, Riverside, California 92521 *(Received: July 9, 1987)*

Formal anisotropic polarizability densities were obtained from quantum charge increments in a small uniform applied field by integrating the general mathematical relation between a charge increment and the divergence of a charge shift polarization. A Gaussian basis set was developed to evaluate the field-induced quantum charge increments. The results for parallel and perpendicular applied fields were fitted to relatively simple Legendre–Laguerre expansions in the elliptic coordinates. Internuclear separation was varied between 1.4 and 3.0 au. The unusual features of H_2^+ relative to H_2 and to diatomics with inner-shell electrons are discussed.

Introduction

The H_2^+ molecule was chosen for initial studies of the distributed anisotropic polarizability of a chemical bond primarily because it is a one-electron system. The time-averaged charge increment at each point depends only on the nature of the electron's motion in the nuclear and applied fields. Coulomb repulsion from other parts of the electron cloud is not a consideration because an electron is essentially a point charge on an atomic scale and does not interact with itself at spatially separated points.

In a formal (mathematical) sense, $\Delta\rho$, the field-induced quantum charge increment at each point of space, can be interpreted as the negative divergence of a polarization **P**:

$$-\nabla\cdot\mathbf{P} = \Delta\rho \qquad (1)$$

P(**r**) represents the dipole moment density of the shifted charge density at point **r** relative to its zero-field position, and eq 1 expresses only conservation of charge: If the charge shift varies across a local region, there will be a net local charge increment. The charge density exists in a time-averaged sense at each point of the molecule (with or without a field), and is evaluated by solving the Schroedinger equation. While the above relation is independent of dielectric theory, the close analogy to it suggests that **P** may be expressed as the product of a formal polarizability density tensor **X** and a small local field **E**. (This is the applied field in the case of a one-electron system.)

Our interest in the continuum dielectric formalism as a model for atomic interiors was stimulated by the work of Oxtoby and Gelbart.[1] A number of other approaches have been explored.[2-9]

(1) (a) Oxtoby, D. W.; Gelbart, W. M. *Mol. Phys.* **1975**, *29*, 1569. (b) *Mol. Phys.* **1975**, *30*, 535. See also: (c) Theimer, O.; Paul, R. *J. Chem. Phys.* **1965**, *42*, 2508. (d) Frisch, H. L.; McKenna, J. *Phys. Rev. A* **1965**, *139*, 68.
(2) (a) Heller, D. F.; Harris, R. A.; Gelbart, W. M. *J. Chem. Phys.* **1975**, *62*, 1947. (b) Cina, J. A.; Harris, R. A. *J. Chem. Phys.* **1984**, *80*, 329.
(3) (a) Applequist, J. *Acc. Chem. Res.* **1977**, *10*, 79. (b) *Chem. Phys.* **1984**, *85*, 279. (c) *J. Chem. Phys.* **1985**, *83*, 809.
(4) Oxtoby, D. W. *J. Chem. Phys.* **1978**, *69*, 1184.

0022-3654/88/2092-2115$01.50/0